

Journal of Engineering Science and Technology
Vol. 13, No. 7 (2018) 2236 - 2245
© School of Engineering, Taylor's University

CONTROL OF A THREE LEVELS AC/DC CONVERTER WITH VIRTUAL-FLUX DIRECT POWER CONTROLLING METHOD FOR GRID-CONNECTED WIND POWER SYSTEM UNDER GRID'S FAULT

A. GAFAZI^{1,2,*}, A. CHEKNANE², I. MERZOUK¹, B. SEDDIK³

¹Applied Automation and Industrial Diagnostic Laboratory,
Faculty of Science and Technology, University of Djelfa, Algeria

²Laboratoire des semi-conducteurs et matériaux fonctionnels,
Université Amar Telidji de Laghouat,
Bd des Martyrs. BP37G, Laghouat 03000, Algeria

³G2Elab, Grenoble INP, France

*Corresponding Author: abdesselamgafazi@gmail.com

Abstract

The present work focuses on modelling of sensor-less Direct Power Control based on Virtual Flux (DPC-VF) for three levels AC/DC converter for wind power system in the case of grid abnormality. As a fact, when an unbalance appears in the grid, the negative sequence affects the quality of Dc-link at the output of the converter and makes deterioration in grid current. In order to improve the behaviour of the converter under grid abnormality, the grid currents and Virtual Flux are decomposed in separating positive and negative sequence using double second order generalized integrator Direct Power Control (DSOGI-FLL) then compensating active and reactive powers are calculated according to the control objective and injected in the referencing one. The proposed controller ensures voltage balance in DC-link capacitors by using redundant vectors in a space vector modulation block without needing additional components. In order to test the effectiveness of the control scheme, a numerical simulation is performed using the Matlab-Simulink software. The results prove the validity of the proposed control algorithm.

Keywords: Direct power control based virtual flux, Double second order generalized integrator, Grid abnormality, Three levels AC/DC converter.

1. Introduction

With the increase of the integration of wind turbines in the grid, many countries have changed their grid code to adapt to this new technology [1, 2]. Under grid fault conditions, the grid code requires wind turbines to remain grid-connected. However, grid faults bring an overcurrent, which can destroy the winding of the generators and/or power converters [3-6]. Thus, the protection of equipment becomes a real issue that brought the attention of researchers in recent years.

In this regard, many researchers are working on developing new algorithms for controlling the grid-connected converter under grid fault to improve its performance and thus protecting the wind energy conversion system [7-13]. These efforts aim to introduce alternatives that can replace the classical methods, which neglect the effects of source voltage unbalance [14-21].

Direct Power Control (DPC) took the largest share of the work done previously [4, 6, 8, 11] because it is simple, robust and gives a good results and can enhance the current grid under grid fault, meanwhile DPC strategies are sensitive for grid distortion, which reduces the applied converter performance, because of the line voltage measured. Thus, the introduction of Virtual Flux to estimate the line voltage is a good alternative for robust operation [12, 22].

The three-level AC/DC converter is more suitable for high power applications and can offer several advantages such as high output voltage with very low distortion, low electromagnetic interference, low DV/DT stresses, and reduced converter losses [14].

This paper proposes a new control scheme for grid-connected converter under grid abnormality in order to get sinusoidal and symmetrical grid current with a fast dynamic response. For that, the referencing current is calculated by the instantaneous power theory. The Virtual Flux is estimated using a DSOGI-FLL method, which is proposed by [10]. The effectiveness of the proposed method has been verified by simulation in MATLAB environment.

The rest of the paper is organized as follows: Section 2 describes the control methods in details. Section 3 presents the simulation results and discussion and finally, the last section are devoted to the main conclusions of the study.

2. Method Description

The structure of three-levels AC/DC converter is illustrated in Fig. 1. Each leg contains four switch and two clamp diodes allow producing three distinct levels.

2.1. Compensation power calculation

Underbalanced grid, the active and reactive power can be calculated using the virtual flux approach from:

$$\begin{cases} P = \frac{3}{2}\omega(\psi_{\alpha}I_{\beta} - \psi_{\beta}I_{\alpha}) \\ Q = -\frac{3}{2}\omega(\psi_{\alpha}I_{\alpha} + \psi_{\beta}I_{\beta}) \end{cases} \quad (1)$$

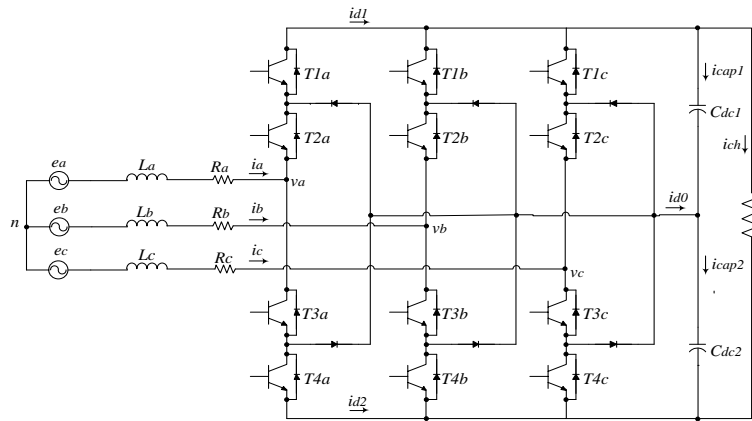


Fig. 1. Three levels ac/dc structure converter.

2.2. Compensation of power calculation

Underbalanced grid, the active and reactive power can be calculated using the virtual flux approach from

$$\begin{cases} P = \frac{3}{2} \omega (\psi_{\alpha} I_{\beta} - \psi_{\beta} I_{\alpha}) \\ Q = -\frac{3}{2} \omega (\psi_{\alpha} I_{\alpha} + \psi_{\beta} I_{\beta}) \end{cases} \quad (1)$$

When an unbalance voltage appears in the grid, the last two equations can be reformulated via symmetrical component theory as follow:

$$\begin{cases} P = \frac{3}{2} \omega (\psi_{\alpha}^{+} I_{\beta}^{+} - \psi_{\beta}^{+} I_{\alpha}^{+} + \psi_{\alpha}^{-} I_{\beta}^{-} - \psi_{\beta}^{-} I_{\alpha}^{-} + \psi_{\alpha}^{0} I_{\beta}^{0} - \psi_{\beta}^{0} I_{\alpha}^{0} + \psi_{\alpha}^{-} I_{\beta}^{+} - \psi_{\beta}^{-} I_{\alpha}^{+}) \\ Q = -\frac{3}{2} \omega (\psi_{\alpha}^{+} I_{\alpha}^{+} + \psi_{\beta}^{+} I_{\beta}^{+} + \psi_{\alpha}^{-} I_{\alpha}^{-} + \psi_{\beta}^{-} I_{\beta}^{-} + \psi_{\alpha}^{0} I_{\alpha}^{0} + \psi_{\beta}^{0} I_{\beta}^{0} + \psi_{\alpha}^{-} I_{\alpha}^{+} + \psi_{\beta}^{-} I_{\beta}^{+}) \end{cases} \quad (2)$$

For the objective to have a sinusoidal and balanced current in the utility grid, we should impose the negative component of current in the Eqs. 3 and 4 to zero; so we get

$$\begin{cases} P = \frac{3}{2} \omega (\psi_{\alpha}^{+} I_{\beta}^{+} - \psi_{\beta}^{+} I_{\alpha}^{+} + \psi_{\alpha}^{-} I_{\beta}^{+} - \psi_{\beta}^{-} I_{\alpha}^{+}) \\ Q = -\frac{3}{2} \omega (\psi_{\alpha}^{+} I_{\alpha}^{+} + \psi_{\beta}^{+} I_{\beta}^{+} + \psi_{\alpha}^{-} I_{\alpha}^{+} + \psi_{\beta}^{-} I_{\beta}^{+}) \end{cases} \quad (3)$$

Compared with the Eq. (1), the compensation power is deduced as:

$$\begin{cases} P_{comp} = \frac{3}{2} \omega (\psi_{\alpha}^{-} I_{\beta}^{+} - \psi_{\beta}^{-} I_{\alpha}^{+}) \\ Q_{comp} = -\frac{3}{2} \omega (\psi_{\alpha}^{-} I_{\alpha}^{+} + \psi_{\beta}^{-} I_{\beta}^{+}) \end{cases} \quad (4)$$

2.3. Virtual Flux estimation

The converter with AC-side voltage sensor can operate with less operation using the concept of Virtual Flux (VF) based approach, which offers two major advantages: the cost reduction by minimizing the number of sensors and natural filtering of line voltage harmonics, and the Virtual Flux at the grid side of the input filter that can be found by integrating the voltage source.

Using the model of PWM AC/DC converter in stationary coordinates shown in Eq. (5).

$$E_{\alpha\beta} = L \frac{di_{\alpha\beta}}{dt} + Ri_{\alpha\beta} + V_{\alpha\beta} \quad (5)$$

The Virtual Flux can be expressed as a result:

$$\psi_{\alpha\beta} = LI_{\alpha\beta} + \int (Ri_{\alpha\beta} + V_{\alpha\beta}) dt \quad (6)$$

To overcome the drawbacks related to the use of cascading filter-method to estimate the Virtual Flux under unbalanced conditions (time delay, sensitivity to grid frequency variation, complex structures and relatively slow transient response). The second order multiple generalised as illustrated in Fig. 2, the integrator Direct Power Control (DSOGI-FLL) is one of the more feasible solutions proposed so far in the literature for its good results in terms of the accuracy and its capability for grid synchronization.

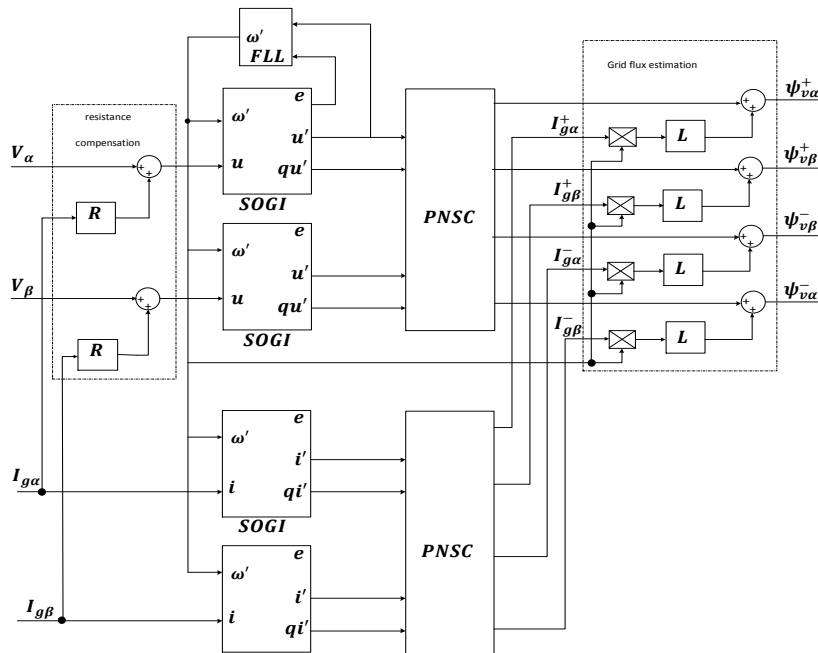


Fig. 2. DSOGI-Based on Virtual Flux estimation.

2.4. Control scheme

The control scheme is decomposed to two loops, the outer loop for dc-link regulation and consequently gives the active power reference; the reference of the reactive power is set to zero to guarantees the unity power factor. The inner loop is reserved to regulate active and reactive powers via two PI controllers where the output gives the referenced voltages to apply in the input of the converter. Finally, an SVM bloc is used to generate the switching function for semiconductor devices. The control strategy is summarized in the block diagram of Fig. 3.

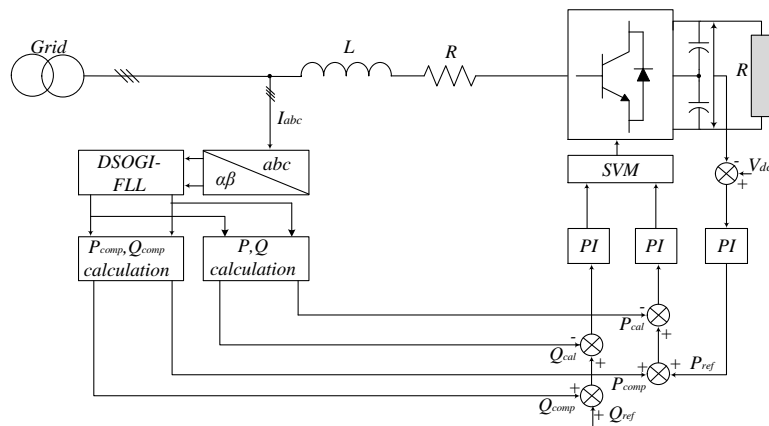


Fig. 3. Block diagram of the proposed control.

3. Simulation and Discussion

The simulation of the proposed control scheme was carried out using Matlab environment. The parameters of the system and grid voltage values are shown in Table 1. The gains of PI regulators are calculated with the symmetrical optimum based design.

Table 1. Test system parameters.

Variable	Symbol	Value
Input filter inductance	L	12 mH
Input filter resistance	R	0.3 Ω
DC-link capacitance	C_{dc}	5000 μF
Load	R_{ch}	100 Ω
DC-link voltage	V_{dc}	2400 V

The proposed control scheme is tested as the voltage changes from the ideal voltage supply to the perturbed one. The distorted voltage supply, in this case, is a 30% decrease of the amplitude of the first phase at the time of 0.8 s. It is noted from Fig. 4, that the classical control strategy offers sinusoidal grid currents under ideal conditions. However, under perturbed voltage supply, it becomes unbalanced and full of low harmonic order component. After the introduction of compensating power of time at 0.85 s, the current is equilibrated without any harmonics. We can observe that the DC link voltage still in its reference and the voltages of high and low capacitance are superposed.

Figure 5 shows that DSOGI-FLL can extract the positive and negative component of Virtual Flux with accurate and fast dynamics. The negative component has no value under the balanced grid and then start to rise to a stable value after approximately two periods from the introduction of the unbalance to the grid.

In order to show the robustness of the method we produce two tests; the first one a DC-link reference has been changed from 2400 V to 2600 V at time 0.5 s. The results are shown in Fig. 6. We observe that the DC-link voltage reaches its new value without affecting the system stability the current increase slightly and then come back to their old value. The second order integrator continues to extract the components of Virtual Flux smoothly.

The second test the value of the load is halved at the instant of 0.5 s. Although the introduction of this perturbation and the operation of the system is not affected as shown in Fig. 7.

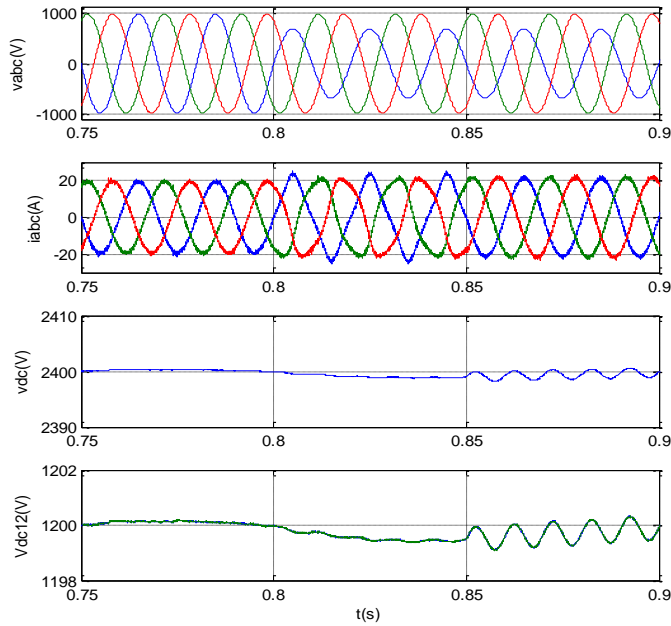


Fig. 4. Simulation result from the top to the bottom line voltage, line current, DC-link voltage and high and low capacitance voltage.

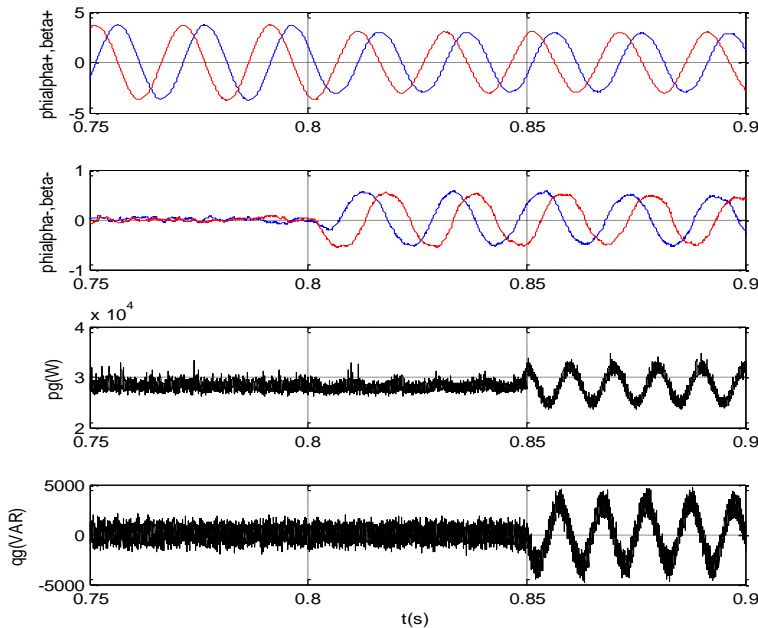


Fig. 5. Simulation result from the top to the bottom positive Virtual Flux, negative Virtual Flux, active power and reactive power.

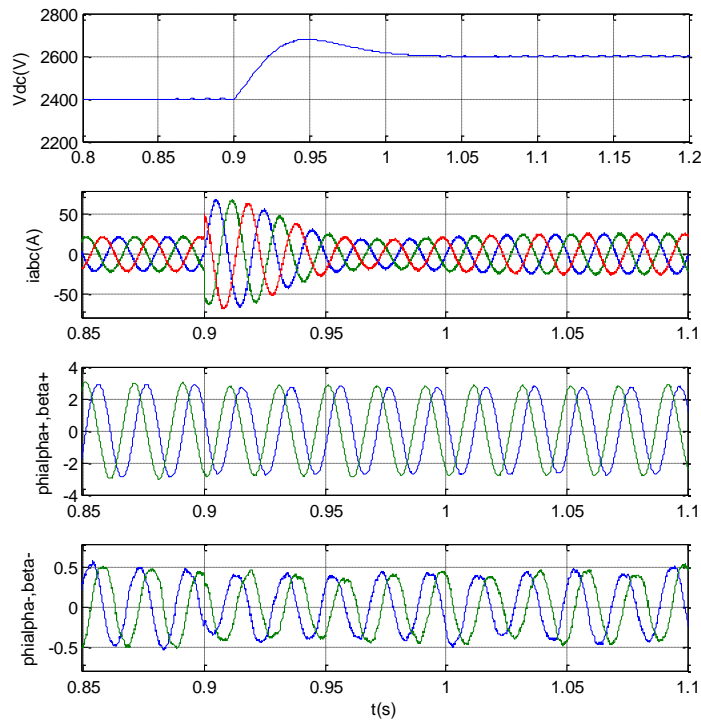


Fig. 6. Simulation result from the top to the bottom DC-link voltage, line current, positive Virtual Flux and negative Virtual Flux.

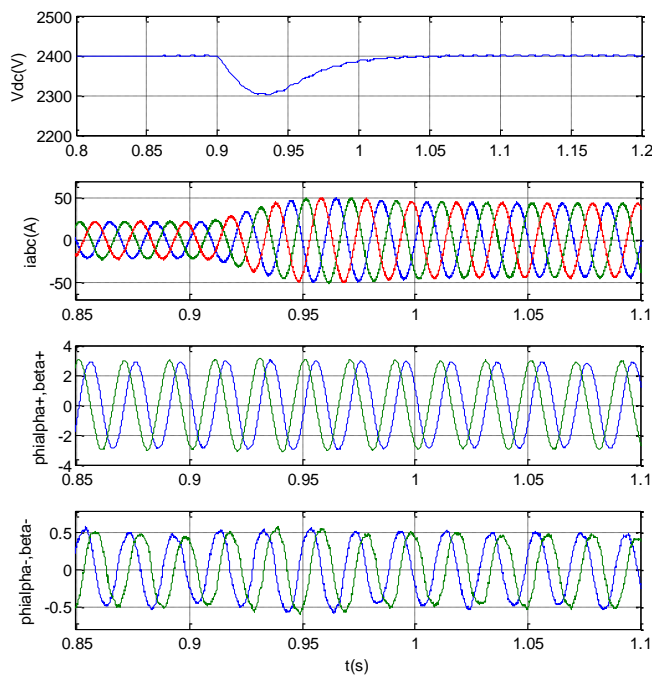


Fig. 7. Simulation result from the top to the bottom. DC-link voltage, line current, positive Virtual Flux and negative Virtual Flux.

4. Conclusions

This paper has proposed a novel structure to compensate control scheme based on improving Virtual Flux Direct Power Control of 3 levels rectifier under unbalanced grid faults. In order to obtain sinusoidal grid currents under unbalanced conditions, compensated powers are calculated and added to the original referenced power to achieve balanced and high-quality grid current.

The modified strategy is verified by simulation under both cases, which are ideal voltage and unbalanced voltage. The DSOGI gives a good solution for grid voltage estimation under grid fault depends on the obtained results. In addition, it proves its capability of yielding sinusoidal grid current with unity power factor under severe non-ideal source.

Nomenclatures

C_{dc}	DC-link capacitor, μF
e_{abc}	Grid phase voltage, V
I_{abc}	Grid current, A
L	Input filter inductance, mH
P	Active power, W
R	Input filter resistance, Ω
Q	Reactive power, Var

Greek Symbols

α, β	Quantities in the stationary Clark reference frame
ψ	Flux, Wb
ω	Grid pulsation, rad/s

Abbreviations

DPC	Direct Power Control
DSOGI	Double Second Order Generalised Integrator
FLL	Frequency Locked Loop
VF	Virtual Flux

References

1. Yang, J.; Fletcher, J.E.; and O'Reilly, J. (2010). A series-dynamic-resistor-based converter protection scheme for doubly-fed induction generator during various fault conditions. *IEEE Transactions on Energy Conversion*, 25(2), 422-432.
2. Davari, M.; and I. Mohamed, Y.A.-R. (2017). Robust DC-link voltage control of a full-scale PMSG wind turbine for effective integration in DC grids. *IEEE Transactions on Power Electronics*, 32(5), 4021-4035.
3. Hu, J.B.; Zhang, W.; Wang, H.-s.; He, Y.K.; and Xu, L. (2009). Proportional integral plus multi-frequency resonant current controller for grid-connected voltage source converter under imbalanced and distorted supply voltage conditions. *Journal of Zhejiang University, Science A*, 10(10), 1532-1540.
4. Shang, L.; Sun, D.; and Hu, J. (2011). Sliding-mode-based direct power control of grid-connected voltage-sourced inverters under unbalanced network conditions. *IET Power Electronics*, 4(5), 570-579.

5. Jiabing, H.; Xu, H.; and He, Y. (2013). Coordinated control of DFIG's RSC and GSC under generalized unbalanced and distorted voltage conditions. *IEEE Transactions on Industrial Electronics*, 60(7), 2808-2819.
6. Nian, H.; and Song, Y. (2014). Direct power control of doubly fed induction generator under distorted grid voltage. *IEEE Transactions on Power Electronics*, 29(2), 894-905.
7. Xiao, P.; Corzine, K.A.; and Venayagamoorthy, G.K. (2008). Multiple reference frame-based control of three-phase PWM boost rectifiers under unbalanced and distorted input conditions. *IEEE Transactions on Power Electronics*, 23(4), 2006-2017.
8. Eloy-Garcia, J.; Arnaltes, S.; and Redriguez-Amenedo, J.L. (2007). Direct power control of voltage source inverters with unbalanced grid voltages. *IET Power Electronics*, 1(3), 395-407.
9. Vincenti, D.; and Jin, H. (1994). A three-phase regulated PWM rectifier with on-line feedforward input unbalance correction control. *Proceedings of the IEEE Canadian Conference on Transactions on Electrical and Computer Engineering*. Vancouver, B.C., Canada, 72-75.
10. Suul, J.A. (2012). *Control of grid-integrated voltage source converters under unbalanced conditions*. Ph.D. Thesis. Faculty of Information Technology, Mathematics and Electrical Engineering, Norwegian University of Science and Technology, Trondheim, Norway.
11. Zhang, Y.; and Qu, C. (2015). Table-based direct power control for three-phase AC/DC converters under unbalanced grid voltages. *IEEE Transactions on Power Electronics*, 30(12), 7090-7099.
12. Jon, A.S.; Luna, A.; Rodriguez, P.; and Undeland, T. (2012). Virtual-flux-based voltage-sensor-less power control for unbalanced grid conditions. *IEEE Transactions on Power Electronics*, 27(9), 4071-4087.
13. Sun, D.; Wang, X., and Fang, Y. (2016). Backstepping direct power control without phase-locked loop of AC/DC converter under both balanced and unbalanced grid conditions. *IET Power Electronics*, 9(8), 1614-1624.
14. Portillo, R.; Vazquez, S.; Leon, J.I.; Prats, M.M.; and Franquelo, L.G. (2013). Model-based adaptive direct power control for three-level NPC converters. *IEEE Transactions on Industrial Informatics*, 9(2), 1148-1157.
15. Choi, D.-K; and Lee, K.-B. (2015). Dynamic performance improvement of AC/DC converter using model predictive direct power control with finite control set. *IEEE Transactions on Industrial Electronics*, 62(2), 757-767.
16. Riviera, S.; Wu, B.; Kouro, S.; Venkata, Y.; Yaramasu, V.; and Wang, J. (2015). Electric vehicle charging station using a neutral point clamped converter with bipolar DC bus. *IEEE Transactions on Industrial Electronics*, 62(4), 1999-2009.
17. Schmidlin Junior, C.R.; and Lima, F.K.A. (2016). Wind turbine and PMSG dynamic modelling in PSIM. *IEEE Latin America Transactions*, 14(9), 4115-4120.
18. Calle-Prado, A.; Alepuz, S.; Bordonau, J.; Cortes, P., and Rodriguez, J. (2016). Predictive control of a back-to-back NPC converter-based wind power system. *IEEE Transactions on Industrial Electronics*, 63(7), 4615-4627.

19. Kulikowski, K.; and Sikorski, A. (2016). New DPC look-up table methods for three-level AC/DC converter. *IEEE Transactions on Industrial Electronics*, 63(12), 7930-7938.
20. Madhusoodhanan, S.; Mainali, K.; Awneesh, Tripathi, A.; Patel, D.; Kadavelugu, A.; Bhattacharya, S.; and Hatua, K. (2017). Harmonic analysis and controller design of 15 kV SiC IGBT-based medium-voltage grid-connected three-phase three-level NPC converter. *IEEE Transactions on Power Electronics*, 32(5), 3355-3369.
21. Eren, S.; Pahlevani, M.; Bakhshai, A.; and Jain, P. (2017). A digital current control technique for grid-connected AC/DC converters used for energy storage systems. *IEEE Transactions on Power Electronics*, 32(5), 3970-3988.
22. Cho, Y.; and Lee, K.-B. (2016). Virtual-flux-based predictive direct power control of three-phase PWM rectifiers with fast dynamic response. *IEEE Transactions on Power Electronics*, 31(4), 3348-3359.

Appendix A

Structure of DSOGI and FLL

The structure of DSOGI is given in Fig. A-1. The constants K and Γ are the damping factor of the filter (determine the performance and the dynamic response of the SOGI) and the gain of Direct Power Control consecutively. The optimum values for k and Γ are $\sqrt{2}$ and 50. To refer to it in obtaining more details [10].

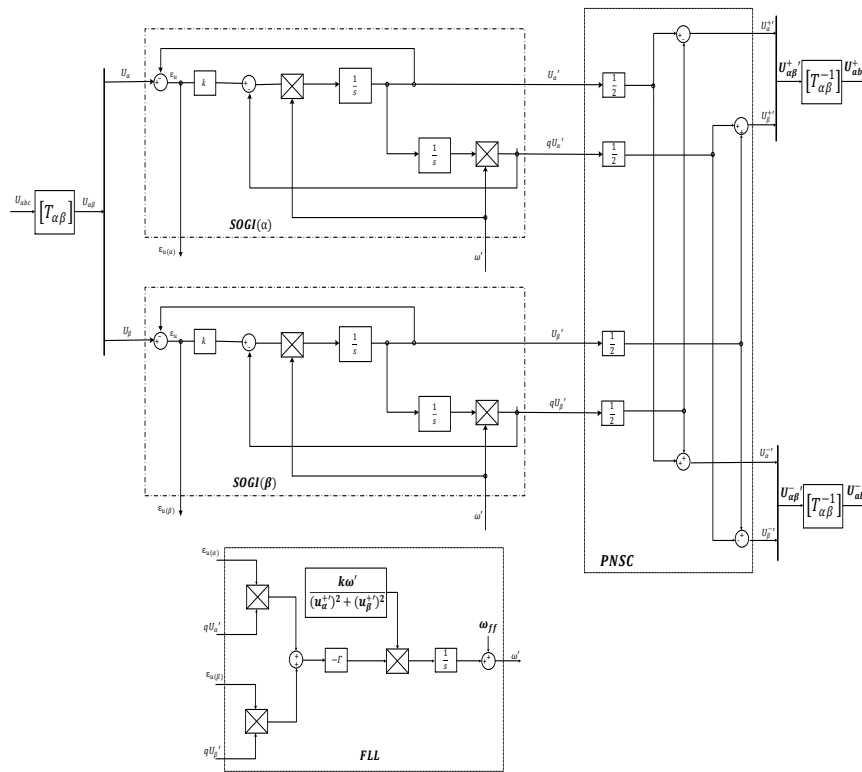


Fig. A-1. Detailed structure of DSOGI and FLL.